ChemComm

Accepted Manuscript

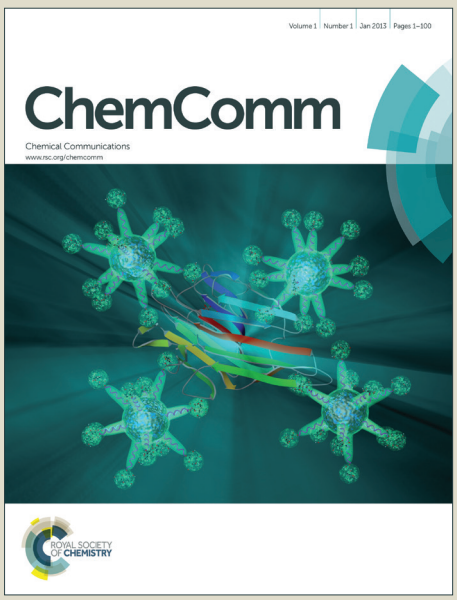

ROYAL SOCIETY OF CHEMISTRY

www.rsc.org/chemcomm

Journal Name

RSCPublishing

COMMUNICATION

Deciphering the Origin of Cooperative Catalysis by Dirhodium Acetate and Chiral Spiro Phosphoric Acid in an Asymmetric Amination Reaction†

Cite this: DOI: 10.1039/xoxxoooooox

Received ooth July 2014,
Accepted ooth

www.rsc.org/

Hemanta K. Kisan and Raghavan B. Sunoj*

The mechanism of asymmetric amination of diazo-acetate by tert-butyl carbamate catalyzed by dirhodium tetra(trifluoro)acetate and chiral SPINOL-phosphoric acid is examined using DFT (M06 and B3LYP) computations. Cooperative participation of both catalysts is noticed in the stereo-controlling transition state of the reaction.

Over the years, chemists have harnessed the catalytic potential of transition metal catalysts[1] as well as organocatalysts.[2] While the independent use of these catalysts continues to flourish, efforts to put together their complimentary attributes have witnessed a steady growth.[3] This methodology, known as cooperative catalysis, holds immense promise.[4] Impressive strides have been made in asymmetric cooperative catalysis in the recent years.[5]

Dirhodium carboxylates have found widespread use in cooperative catalysis.[6] Although carbenoids derived from dirhodium carboxylates have been around for a while as a synthetic precursor,[7] the significant recent developments engender renewed focus on its chemistry.[8] Similarly, widely known C–N bond formation reactions rely on carbene insertion into the N–H bond using dirhodium (II) carboxylates.[9] Very recently, Zhou and coworkers demonstrated that carbene insertion to *tert*-butyl carbamate ($BocNH_2$) can offer *α*-amino ester with enantioselectivities of the order of 95% (Scheme 1).[10] Here, α-diazo-α-phenylacetate **1** serves as the carbene precursor whereas chiral source for asymmetric N–H insertion emanates from spiro phosphoric acid (*R*)-SPA. Although the most common genre of asymmetric catalysis using dirhodium carbenoids employs chiral bridging ligands,[11] it appears that the present reaction relies on the cooperative/tandem catalysis offered by a chiral Brønsted acid.

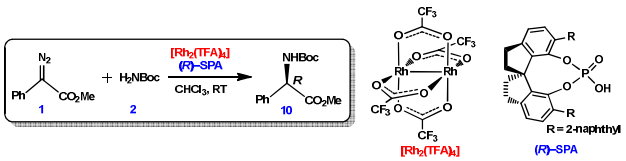

Scheme 1. Asymmetric N–H insertion reaction catalyzed by dirhodium (II) tetra(trifluoroacetate) $[Rh_2(TFA)_4]$ and chiral spiro phosphoric acid (R)-SPA (ref. 10)

Department of Chemistry, Indian Institute of Technology Bombay, Powai, Mumbai 400076, India. Email: sunoj@chem.iitb.ac.in

† Electronic supplementary information (ESI): Full computational details and optimized Cartesian coordinates are provided. See DOI: 10.1039/c000000x/

In the experimental procedure, both dirhodium(II) tetra(trifluoro)acetate $[Rh_2(TFA)_4]$ and SPINOL phosphoric acid (*R*)-SPA (SpiroIndanediol based phosphoric acid) are mixed in chloroform. The reactants, namely, methyl *α*-diazo-*α*-phenylacetate (**1**) and *tert*-butyl carbamate (**2**, $BocNH_2$) is subsequently introduced in one portion.[10] Under such conditions, different combinations of reactants and catalysts can be envisaged.[12] Mechanistic studies on such multi-catalytic reactions are seldom reported. Timely mechanistic rationalization would help exploit the potential of such multi-catalytic asymmetric methodologies. In continuation of our interest in asymmetric catalysis,[13] we have employed M06 and B3LYP density functional theory methods to probe the mechanism of the title reaction between **1** and **2** in the presence of $[Rh_2(TFA)_4]$ and (*R*)-SPA.[14] In particular, we intend to identify whether the action of the two catalysts occurs in sequence (tandem) or simultaneous (cooperative) in the catalytic cycle. These are significantly important questions in light of the burgeoning activities in cooperative catalysis.

The reaction can broadly be considered as proceeding through steps shown in Scheme 2 involving (i) the activation and extrusion of a molecule of nitrogen from the diazoester (**1**) leading to an electrophilic dirhodium carbenoid intermediate (**5**), (ii) the C–N bond formation between the carbenoid and *tert*-butyl carbamate (**2**), (iii) enolization and release of an enol intermediate (**7**), and finally (iv) enantioselective protonation of the enol intermediate leading to a chiral *α*-amino ester as the product. The relative Gibbs free energies of various stationary points involved in the formation of enol intermediate (**7**) is provided in Scheme 2. Whereas the initial interaction between the diazoacetate and dirhodium is generally considered to involve a C-coordination (**4**), we note that the initial coordination through the ester oxygen of the diazo ester (**3**), followed by a change of coordination from O to C via the transition state **(3-4)**‡ to a 1,3-dipolar intermediate (**4**) is energetically feasible. In the next step, the activation of the diazo ester (**1**) and nitrogen extrusion takes place through **(4-5)**‡. The resulting exoergic dirhodium carbenoid (**5**) occupies a central position in the mechanistic course of this reaction. Interestingly, an equivalent dirhodium carbenoid (**5**) has very recently been isolated.[8b]

The electrophilic carbenoid **5** will now react with *tert*-butyl carbamate (**2**) in the next step. The transition state **(5-6)**‡ is found to be of low energy.[15] The 1,3-dipolar intermediate **6**(or **6'**, which refers to the opposite configuration at the *α*-carbon) thus generated can undergo either (i) a proton transfer from the amino- to the ester-

group to provide an enol intermediate ((*Z*)-enol(**7**), (*E*)-enol(**7'**), Scheme 3(a)) or (ii) a change of coordination of rhodium from the carbenic carbon to the ester oxygen to give the generally proposed dirhodium enolate ((*Z*)-enolate(**8**), (*E*)-enolate(**8'**), (Scheme 3(b)) or (iii) a change in coordination of rhodium from the carbenic carbon to the carbonyl oxygen of the N-Boc group to give an ylide (**9**) (Scheme 3(c)). All the key geometric arrangements arising due to different configurations at the carbon atom bound to the rhodium as well as around the enol(ate) double bond are examined so as to identify the most preferred pathway for the generation of enol(ate).[16] It is noted that an intramolecular proton transfer via TS **(6-7)‡** leading to *E*-enol (**7**) is energetically the most preferred route. This intramolecular protonation is accompanied by a concomitant departure of the [$Rh_2(TFA)_4$] by Rh–C bond breaking, providing a free enol for the subsequent steps of the reaction (Scheme 3(a)).[17] The TS for an alternative path, wherein (*R*)-SPA participates in a relay proton transfer leading to a *Z*-enol (**7'**), is found to be more than 10 kcal/mol higher in energy (Scheme 3, **(6-7)‡** and **(6-7')‡**).[18]

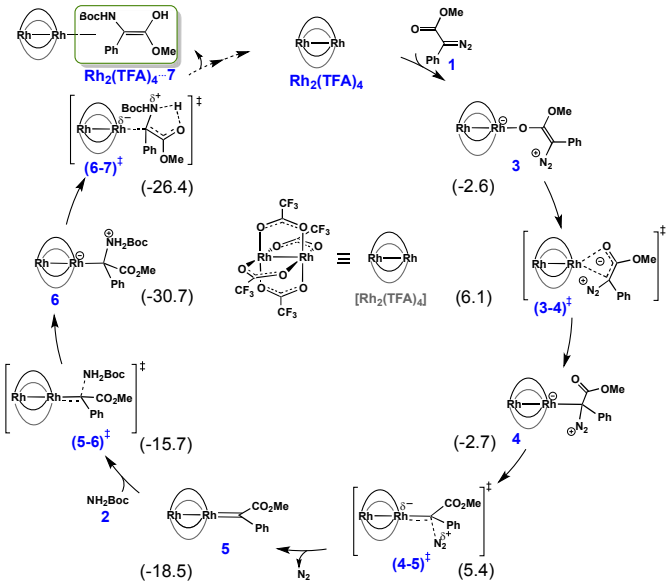

Scheme 2. Key steps in [$Rh_2(TFA)_4$] catalyzed reaction between diazoacetate and *tert*-butyl carbamate. The relative Gibbs free energies (kcal/mol) with respect to the separated reactants provided in parenthesis computed at the $SMD_{(chloroform)}$/M06//B3LYP/Lanl2DZ(Rh),6-31G** level of theory.

The most interesting feature emerging at this juncture is the computed energetic advantage for the formation of an enol (**7**) over a dirhodium enolate (**8**) and an ylide (**9**). Almost all mechanistic studies thus far have proposed the involvement of either a dirhodium enolate or an ylide as the key intermediate. We noticed that the TS for the change of coordination from carbon to oxygen (**(6-8)‡** or **(6'-8')‡**) which is responsible for the generation of dirhodium enolates (**8**/**8'**) are more than 24 kcal/mol higher in energy than that for the enol formation via **(6-7)‡** (Scheme 3(b)).[16] The TS for the formation of enols **7** and **7'** are lower in energy respectively by 24.4 and 14 kcal/mol as compared to that leading to enolate **8**. This is evident by comparing the energies of **(6-7)‡** and **(6-7')‡** with that of **(6-8)‡** (Scheme 3). Equally important is to note that the TS for ylide generation **(6-9)‡** is 27.2 kcal/mol higher than that for enol (**7**) formation (Scheme 3(c)). Additionally, the resulting dirhodium enolates (**8**/**8'**), dirhodium ylide (**9**···[$Rh_2(TFA)_4$]) and free ylide (**9**) all are of higher energy as compared to the free enol (**7**) as well as the dirhodium-bound enol intermediates (**7**···[$Rh_2(TFA)_4$]).[16]

Table 1. The Computed Relative Gibbs Free Energies (in kcal/mol) for the Key Intermediates and the Transition states

Entry	Stationary Point	ΔG1	ΔG2	ΔG3
1	**3**	0.6	1.0	-2.6
2	**(3-4)‡**	14.9	13.7	6.1
3	**4**	10.5	9.8	-2.7
4	**(4-5)‡**	18.9	17.4	5.4
5	**5**	-9.9	-10.6[a]	-18.5
6	**(5-6)‡**	2.2	0.1	-15.7
7	**6**	-13.2	-14.9	-30.7
8	**(6-7)‡**	-10.4	-11.9	-24.6
9	**(6-8)‡**	6.7	6.4	-2.0

The ΔG1 and ΔG2 respectively indicate the relative Gibbs free energies obtained in the condensed phase (in chloroform solvent) at the $B3LYP_{(chloroform)}$/DGDZVP(Rh),6-31G**(C,H,N,O,F) and at the $B3LYP_{(Chloroform)}$/Lanl2DZ(Rh),6-31G**(C,H,N,O,F) level of theories. [a] single-point energy on the gas phase geometry. The ΔG3 indicates the relative Gibbs free energies obtained by using the single-point energy calculations at the $SMD_{(Chloroform)}$/M06/Lanl2DZ(Rh),6-31G**(C,H,N,O,F,P,Cl) level of theory on the B3LYP/Lanl2DZ(Rh), 6-31G*(C,H,N,O,F) geometry in the gas phase.

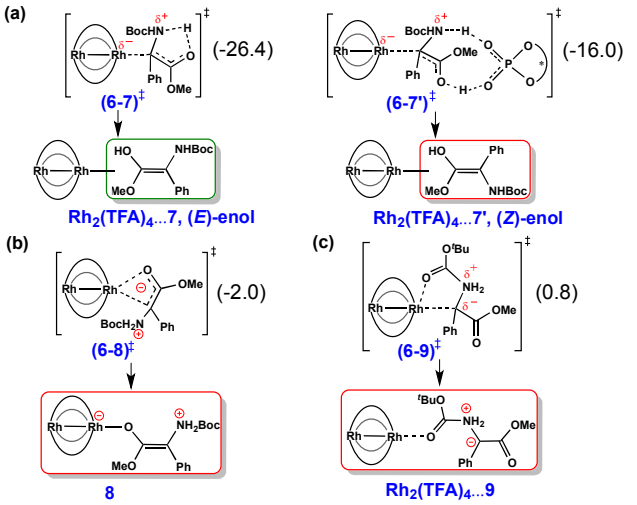

Scheme 3. Different transition states for enolization (**7**/**7'** or **8**) and for the generation ylide (**9**) from the 1,3-dipolar intermediate (**6**). The relative Gibbs free energies (kcal/mol) provided in parenthesis computed at the $SMD_{(chloroform)}$/M06//B3LYP/Lanl2DZ(Rh),6-31G** level of theory.

The most important step in the reaction is the enantioselective protonation of the *α*-carbon to furnish a chiral *α*-amino ester. Depending on the proton source as well as the mode of protonation, different scenarios can be envisaged (Scheme 3).[19] The direct intramolecular 1,2-proton transfer in the 1,3-dipolar intermediate **6** (or **6'**) can result in the final product **10**. However, the TS for proton transfer from the amino nitrogen to the *α*-carbon by both direct as well as relay transfer by (*R*)-SPA are found to be respectively 39.2 and 25.0 kcal/mol higher as compared to the formation of the enol intermediate via **(6-7)‡**.[20] In view of this situation, we have considered number of additional possibilities for the stereoselective protonation of the *α*-carbon of the enol (**7** or **7'**) by chiral (*R*)-SPA.[21]

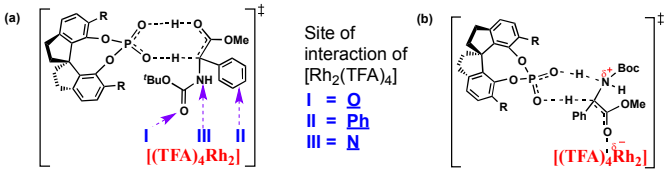

Fig 1. Stereocontrolling transition states involving double proton transfer to (a) (*E*)-enol (**7**) or **7**…[$Rh_2(TFA)_4$, and (b) enolate (**8**/**8'**) intermediates.

As noted earlier the enol intermediate (**7**/**7'**) or the dirhodium enolate (**8**/**8'**) can as well undergo stereoselective protonation to the *si* and *re* prochiral faces to provide the final product (Fig 1). The interaction of dirhodium acetate with all the electron rich sites of the enol intermediate (**7**/**7'**) and the corresponding protonation TS in dirhodium-enol intermediates are considered (Fig 1(a)).[16] The relative energies of the important TS, provided in Table 2, indicate that the lowest energy TS is the one when the dirhodium acetate is bound to the carbonyl oxygen of the *N*-Boc group **(7-10)**‡ (entry 2 in Table 2, Fig 1(a)). Another mode wherein dirhodium acetate interacts with the π-face of the *β*-aryl group of the enol is only 3.5 kcal/mol higher than **(7-10)**‡.[21] Most importantly, the protonation TS either to the *si* or *re* prochiral face of the enol **(7-10)**‡ or **(7-10')**‡, with a bound dirhodium acetate, are about 7 kcal/mol lower as compared to its absence (entries 2 and 1 in Table 2).[21] This evidently suggests a cooperative action of both dirhodium and (*R*)-SPA in the stereo-controlling step of the reaction. Interestingly, the Gibbs free energies of the TS for the enantioselective protonation of dirhodium enolates (**8**/**8'**) by (*R*)-SPA are, in general, higher by about 10 kcal/mol than in the corresponding enol-dirhodium pathway (entries 5 and 6 versus 2 in Table 2).[21]

Table 2. Relative Gibbs Free Energies[a] of the Stereocontrolling TSs Involving Relay Proton Transfer by (*R*)-SPA

Entry	Intermediate	*si*-face **(7-10)**‡	*re*-face **(7-10')**‡	Predicted enantiomer
1	**7**	-17.3 (-33.1)	-12.4 (-27.8)	*R*
2	**7O**···$Rh_2(TFA)_4$	-24.4 (-56.9)	-17.0 (-49.4)	*R*
3	**7Ph**···$Rh_2(TFA)_4$	-20.9 (-51.4)	-15.8 (-47.9)	*R*
4	**7N**···$Rh_2(TFA)_4$	-9.4 (-47.2)	-12.7 (-47.1)	*S*
5[b]	**8** ((*Z*)-enolate)	-14.2 (-47.1)	-10.7 (-47.9)	*R*
6[c]	**8'** ((*E*)-enolate)	-12.1 (-46.2)	-12.6 (-47.6)	*S*

[a] In kcal/mol, with respect to the separated reactants computed at the $SMD_{(chloroform)}$/M06//B3LYP/Lanl2DZ(Rh),6-31G** level of theory. The relative electronic energies are in provided in parenthesis. The site of coordination is emphasized by underline [b] Corresponds to **(8-10)**‡ and **(8-10')**‡. [c] Corresponds to **(8'-10)**‡ and **(8'-10')**

To gain insights into the process of asymmetric induction, the TS involving a stereoselective protonation of **7O**···$Rh_2(TFA)_4$ by (*R*)-SPA are analyzed both in the gas phase and in the condensed phase, across different DFT functionals (Fig 2, Table 3).[14] The one and only chiral source, namely (*R*)-SPA, is found to remain closer to the developing chiral carbon center enabling an effective transfer of chirality. A double proton transfer is noticed wherein the phosphoric acid donates its proton to the prochiral carbon at one end of **7O**···$Rh_2(TFA)_4$ while it abstracts the enol proton from the other end. The efficiency of N-H···π and C-H···π weak nonbonding interactions,[22] denoted as a and b in the Fig 2, is higher in **(7-10))**‡ than in **(7-10'))**‡.[23] Similarly, the hydrogen bonding between the dirhodium CF_3 groups and the binaphthyl C–H bonds (c to g) exhibited improved interaction in **(7-10))**‡ as compared to that in **(7-10'))**‡. The cooperative action of both catalysts is thus quite evident in these stereocontrolling TS structures.

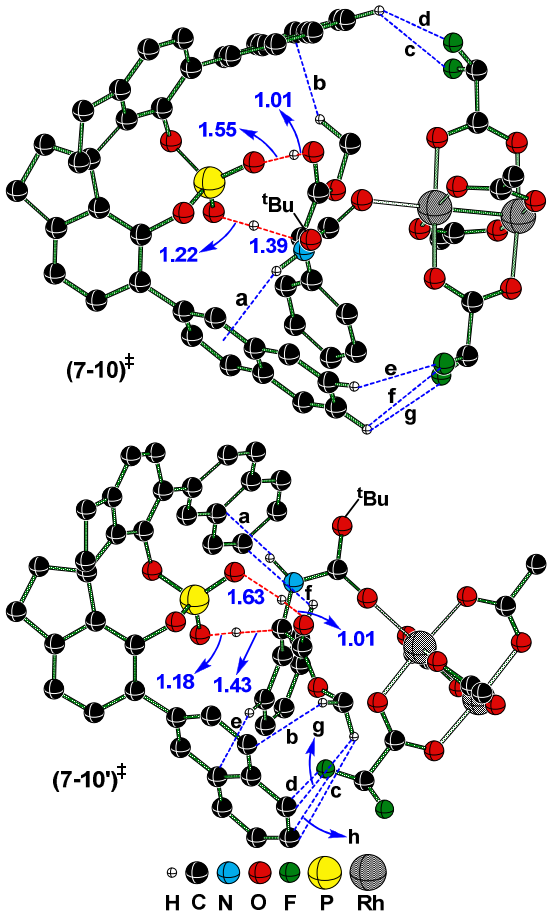

	(7-10)‡			(7-10')‡		
	M06(sol)	B3LYP-D(sol)	B3LYP-D(sol)*	M06(sol)	B3LYP-D(sol)	B3LYP-D(sol)*
a	2.41	2.49	2.53	2.59	2.52	2.69
b	2.69	2.60	2.67	2.64	2.69	2.67
c	2.68	2.62	3.52	2.96	3.24	3.37
d	2.69	2.71	2.66	3.38	3.65	3.61
e	2.86	2.74	4.48	2.96	2.77	2.97
f	3.00	2.74	3.31	3.07	2.79	3.26
g	2.83	2.46	3.33	2.96	2.74	2.82
h	-	-	-	3.00	3.04	3.09

* the distances in red are calculated by using DGDZVP basis set for all the atoms

Fig 2. The stereocontrolling transition state geometries for the enantioselective protonation of the α-carbon of the enol (**7**···[$Rh_2(TFA)_4$]) by (*R*)-SPA optimized at $M06_{(chloroform)}$/Lanl2DZ(Rh),6-31G** level of theory. Distances (a to h) are in Å. Only selected C, H, and F are shown.

Table 3. Relative Gibbs Free Energies (in kcal/mol) of the Stereocontrolling transition states Involving a Relay Proton Transfer by (*R*)-SPA optimized using different DFT functionals

Entry	Level of Theory	*si*-face (ΔG) **(7-10)**‡	*re*-face (ΔΔG) **(7-10')**‡
1[a]	$M06_{(gas)}$	0.0	6.0
2[a]	$B3LYP\text{-}D_{(gas)}$	0.0	9.5
3[a]	$M06_{(sol)}$	0.0	2.6
4[a]	$B3LYP\text{-}D_{(sol)}$	0.0	8.1
5[a, b]	$B3LYP_{(sol)}$	0.0	3.0
6[c]	B3LYP-D(sol)	0.0	6.3

[a] Lanl2DZ for Rh and 6-31G** for rest of the atoms. [b] DGDZVP for Rh and 6-31G** for the rest of atoms. [c] DGDZVP for all atoms.

In conclusion, the cooperative catalytic action of [$Rh_2(TFA)_4$] and (*R*)-SPA is established in the enantioselective protonation of the

amino enol intermediate. The predicted enantioselectivity is in good agreement with the experimentally known values.

Computing time from the IIT Bombay supercomputing facility, senior research fellowship (HKK) from CSIR (New Delhi), and research funding from BRNS (Mumbai) are acknowledged.

Notes and references

1 (a) X.-F. Wu, X. Fang, L. Wu, R. Jackstell, H. Neumann and M. Beller, *Acc. Chem. Res.,* 2014, ***47*, 1041.** (b) Q. Xiao, Y. Zhang and J Wang, *Acc. Chem. Res.,* 2013, ***46***, 236.

2 (a) D. W. C. MacMillan, *Nature,* 2008, ***455***, 304. (b) S. J. Ryan, L. Candish and D. W. Lupton, *Chem. Soc. Rev.,* 2013, ***42***, 4906. (c) A. G. Doyle and E. N. Jacobsen, *Chem. Rev.,* 2007, ***107***, 5713.

3 (a) H. Xu, S. J. Zuend, M. G. Woll, Y. Tao and E. N. Jacobsen, *Science,* 2010, ***327***, 986. (b) D. H. Paul, C. J. Abraham, M. T. Scerba, E. Alden-Danforth and T. Lectka, *Acc. Chem. Res.,* 2008, ***41***, 655.

4 (a) I. Ibrahem and A. Córdova, *Angew. Chem. Int. Ed.,* 2006, ***45***, 1952. (b) N. Kumagai and M. Shibasaki, *Angew. Chem. Int. Ed.,* 2011, ***50***, 4760. (c) B. Xu, S.-F. Zhu, X.-D. Zuo, Z.-C. Zhang and Q.–L. Zhou, *Angew. Chem. Int. Ed.,* 2014, ***53***, 3913.

5 (a) D. Monge, K. L. Jensen, P.T. Franke, L. Lykke and K. A. Jørgensen, *Chem. Eur. J.,* 2010, ***16***, 9478. (b) S. Zhou, S. Fleischer, K. Junge and M. Beller, *Angew. Chem. Int. Ed.,* 2011, ***50***, 5120.

6 (a) H. M. L. Davies, *Angew. Chem. Int. Ed.,* 2006, ***45***, 6422. (b) M. Terada and Y. Toda, *Angew. Chem. Int. Ed.,* 2012, ***51***, 2093. (c) H. Qiu, M. Li, L.-Q. Jiang, F.-P. Lv, L. Zan, C.-W. Zhai, M. P. Doyle and W.-H. Hu, *Nature Chem.,* 2012*, **4**,* 733.

7 (a) A. V. Gulevich and V. Gevorgyan, *Angew. Chem. Int. Ed.,* 2013, ***52***, 1371. (b) N. Selander, B. T. Worrell and V. V. Fokin, *Angew. Chem. Int. Ed.,* 2012, ***51***, 13054.

8 (a) H. M. L. Davies and J. R. Manning, *Nature,* 2008, ***451***, 417. (b) K. P. Kornecki, J. F. Briones, V. Boyarskikh, F. Fullilove, J. Autschbach, K. E. Schrote, K. M. Lancaster, H. M. L. Davies and J. F. Berry, *Science,* 2013, ***342***, 351.

9 (a) C. Bolm, A. Kasyan, K. Drauz, K. Gunther and G. Raabe, *Angew. Chem. Int. Ed.,* 2000, ***39***, 2288. (b) B. Shi, A. J. Blake, W. Lewis, I. B. Campbell, B. D. Judkins and C. J. Moody, *J. Org. Chem*., 2010, ***75***, 152.

10 B. Xu, S.-F. Zhu, X.-L. Xie, J.-J. Shen and Q.-L. Zhou, *Angew. Chem. Int. Ed.,* 2011, ***50***, 11483.

11 (a) H. M. L. Davies, *Angew. Chem. Int. Ed.,* 2006, ***45***, 6422. (b) S. Chuprakov, J. A. Malik, M. Zibinsky and V. V. Fokin, *J. Am. Chem. Soc.,* 2011, ***133***, 10352.

12 Energetic details of catalyst-substrate adducts are provided in Figure S1 in the ESI.

13 (a) G. Jindal and R. B. Sunoj, *Angew. Chem. Int. Ed.,* 2014, ***53***, 4432. (b) A. K. Sharma and R. B. Sunoj, *Angew. Chem. Int. Ed.,* 2010, ***49***, 6373.

14 (a) Gibbs free energies in the solvent are computed at the $SMD_{(chloroform)}$/M06//B3LYP/Lanl2DZ(Rh),6-31G** level using Gaussian09, M. J. Frisch, *et al.* See the ESI for full details. (b) The stereodetermining transition states were re-optimized both in the gas phase and in the condensed phase using different DFT functionals, including DGDZVP basis set for all atoms (B3LYP-D).

15 (a) Among the additions to both the faces of the carbenic carbon, only the lower energy one is presented here. (b) Geometries and additional modes *tert*-butyl carbamate addition to **5** are given in Figure S2 in the ESI.

16 Additional details are provided in Table S1/Figure S3 in the ESI.

17 See Figure S4 and Table S1 in the ESI. A systematic increase in the Rh-C distance toward the product side of the TS in the IRC run, indicating the expulsion of $Rh_2(TFA)_4$. The dirhodium can continue to maintain weak interaction with the donor atoms on enol (O=C(^{t}Boc), $NH_2{}^t$Boc, Ph group, or C=C of the enol).

18 Examples on relay proton transfer See M. Anand and R. B. Sunoj, *Phys. Chem. Chem. Phys.,* 2012, ***14***, 12715.

19 A full set of possibilities is provided in Table S2 in the ESI.

20 Additional details are provided in Figure S5 in the ESI.

21 For details of these TSs, see Figures S6 and S7 in the ESI.

22 The ρ(bcp) obtained using the AIM formalism provides additional support. See Table S3 in the ESI.

23 Two additional interaction in **(7-10')‡** (^{t}Boc C-H···O(P-O) and ^{t}Boc C-H···O(P=O) keep the ^{t}Boc closer to the center of the chiral cavity (Figure S8 in the ESI).

